Fabrication and testing of planar chalcogenide waveguide integrated microfluidic sensor

Juejun Hu, Vladimir Tarasov, Anu Agarwal, and Lionel Kimerling

Microphotonics Center, Massachusetts Institute of Technology
anu@mit.edu

Nathan Carlie, Laeticia Petit, and Kathleen Richardson

Advanced Materials Research Laboratory, Clemson University

Abstract: We have fabricated and tested, to the best of our knowledge, the first microfluidic device monolithically integrated with planar chalcogenide glass waveguides on a silicon substrate. High-quality $Ge_{23}Sb_7S_{70}$ glass films have been deposited onto oxide coated silicon wafers using thermal evaporation, and high-index-contrast channel waveguides have been defined using SF_6 plasma etching. Microfluidic channel patterning in photocurable resin (SU8) and channel sealing by a polydimethylsiloxane (PDMS) cover completed the device fabrication. The chalcogenide waveguides yield a transmission loss of 2.3 dB/cm at 1550 nm. We show in this letter that using this device, N-methylaniline can be detected using its well-defined absorption fingerprint of the N-H bond near 1496 nm. Our measurements indicate linear response of the sensor to varying N-methylaniline concentrations. From our experiments, a sensitivity of this sensor down to a N-methylaniline concentration 0.7 vol. % is expected. Given the low-cost fabrication process used, and robust device configuration, our integration scheme provides a promising device platform for chemical sensing applications.

OCIS codes: (130.6010) Sensors; (130.3120) Integrated optics devices; (230.7390) Waveguides, planar; (300.1030) Absorption.

References and links

1. E. Verpoorte and N. De Rooij, "Microfluidics meets MEMS," Proc. IEEE. **91**, 930-953 (2003).
2. P. Friis, K. Hoppe, O. Leistiko, K. Mogensen, J. Hubner, and J. Kutter, "Monolithic integration of microfluidic channels and optical waveguides in silica on silicon," Appl. Opt. **40**, 6246-6251 (2001).
3. N. Petersen, K. Mogensen, and J. Kutter, "Performance of an in-plane detection cell with integrated waveguides for UV/Vis absorbance measurements on microfluidic separation devices," Electrophoresis **23**, 3528-3536 (2002).
4. L. Zhu, Y. Huang, and A. Yariv, "Integrated microfluidic variable optical attenuator," Opt. Express **13**, 9916-9921 (2005).
5. T. Galstyan, J. Viens, A. Villeneuve, K. Richardson, and M. Duguay, "Photoinduced self-developing relief gratings in thin film chalcogenide As_2S_3 glasses," J. Lightwave Technol. **15**, 1343-1347 (1997).
6. Z. Sun, J. Zhou, and R. Ahuja, "Structure of phase change materials for data storage," Phy. Rev. Lett. **96**, 055507 (2006).
7. A. Ozols, D. Saharovs, and M. Reinfelde, "Holographic recording in amorphous As_2S_3 films at 633 nm," J. Non-Cryst. Sol. **352**, 2652-2656 (2006).
8. W. Chung, H. Seo, B. Park, J. Ahn, and Y. Choi, "Selenide glass optical fiber doped with Pr^{3+} for U-band optical amplifier," Etri Journal **27**, 411-417 (2005).
9. A. Mairaj, C. Riziotis, A. Chardon, P. Smith, D. Shepherd, and D. Hewak, "Development of channel waveguide lasers in Nd^{3+}-doped chalcogenide (Ga:La:S) glass through photoinduced material modification," Appl. Phys. Lett. **81**, 3708-3710 (2002).
10. X. Zhang, L. Calvez, V. Seznec, H. Ma, S. Danto, P. Houizot, C. Boussard-Pledel, and J. Lucas, "Infrared transmitting glasses and glass-ceramics", J. Non-Cryst. Sol. **352**, 2411-2415 (2006).

#78720 - $15.00 USD Received 4 January 2007; revised 5 February 2007; accepted 19 February 2007

11. C. Kerbage, A. Hale, A. Yablon, R. Windeler, and B. Eggleton, "Integrated all-fiber variable attenuator based on hybrid microstructure fiber," Appl. Phys. Lett. **79**, 3191-3193 (2001).
12. P. Mach, M. Dolinski, K. Baldwin, J. Rogers, C. Kerbage, R. Windeler, and B. Eggleton, "Tunable microfluidic optical fiber," Appl. Phys. Lett. **80**, 4294-4296 (2002).
13. O. Efimov, L. Glebov, K. Richardson, E. Van Stryland, T. Cardinal, S. Park, M. Couzi, and J. Bruneel, "Waveguide writing in chalcogenide glasses by a train of femtosecond laser pulses," Opt. Mater. **17**, 379-386 (2001).
14. J. Viens, C. Meneghini, A. Villeneuve, T. Galstian, E. Knystautas, M. Duguay, K. Richardson, and T. Cardinal, "Fabrication and characterization of integrated optical waveguides in sulfide chalcogenide glasses," J. Lightwave Technol. **17**, 1184-1191 (1999).
15. Y. Ruan, W. Li, R. Jarvis, N. Madsen, A. Rode, and B. Luther-Davies, "Fabrication and characterization of low loss rib chalcogenide waveguides made by dry etching," Opt. Express **12**, 5140-5145 (2004).
16. J. Hu, V. Tarasov, A. Agarwal, and L. Kimerling, Microphotonics Center, Massachusetts Institute of Technology, 77 Mass Ave, Cambridge, M.A. 02139 and N. Carlie, L. Petit, K. Richardson are preparing a manuscript to be called "Waveguide Fabrication From Thermally Evaporated Ge-Sb-S Glass Films."
17. A. Ganjoo, H. Jain, C. Yu, R. Song, J. Ryan, J. Irudayaraj, Y. Ding, and C. Pantano, "Planar chalcogenide glass waveguides for IR evanescent wave sensors," J. Non-Cryst. Sol. **352**, 584-588 (2006).
18. L. Petit, N. Carlie, F. Adamietz, M. Couzi, V. Rodriguez, and K. C. Richardson, "Correlation between physical, optical and structural properties of sulfide glasses in the system Ge-Sb-S," Mater. Chem. Phys. **97**, 64-70 (2006).
19. R. DeCorby, N. Ponnampalam, M. Pai, H. Nguyen, P. Dwivedi, T. Clement, C. Haugen, J. McMullin, and S. Kasap, "High index contrast waveguides in chalcogenide glass and polymer," IEEE J. Sel. Top. Quantum Electron. **11**, 539-546 (2005).
20. C. Xu, W. Huang, M. Stern, and S. Chaudhuri, "Full-vectorial mode calculation by finite difference method," IEE Proc. Optoelectron., **141**, 281–286 (1994).
21. S. Shaji, S. Eappen, T. Rasheed, and K. Nair, "NIR vibrational overtone spectra of N-methylaniline, N,N-dimethylaniline and N,N-diethylaniline - a conformational structural analysis using local mode model," Spectrochim. Acta, Part A, **60**, 351-355 (2004).
22. J. Hu, V. Tarasov, N. Carlie, R. Sun, L. Petit, A. Agarwal, K. Richardson, and L. Kimerling, "Low-loss integrated planar chalcogenide waveguides for chemical sensing," Proc. SPIE **6444** (to be published).
23. V. Zolotarev, B. Mikhilov, L. Alperovich, S. Popov, "Dispersion and absorption of liquid water in the infrared and radio regions of the spectrum," Opt. Spectrosc. **27**, 430-432 (1969).

1. Introduction

An actively investigated area since its debut in the early 1990s, microfluidics has been an emerging concept that can potentially revolutionize chemical and biological analysis. The development of microfluidic chips, platforms comprising micro-channel systems connecting liquid reservoirs, envisions the integration of sample preparation, separation, purification, and identification functionalities onto one single chip, i.e. the so-called "lab-on-a-chip" concept. Such miniaturized systems are amenable to mass production, enabling highly complex flow systems and automated, multiplexed analysis with minimal analyte volumes, significantly reducing cost and human intervention [1]. Given the advantages of microfluidic analytical chips over their conventional macroscopic counterparts, efforts have been made to integrate microfluidic systems with planar optical waveguides for spectroscopic sensing [2, 3] and optical attenuators [4]. Advantages of such systems include low cost, robustness, the possibility of integration with peripheral electronics, long optical path length, and hence significantly improved sensitivity. However, the waveguide materials that have been used for this purpose are silicon oxide or oxynitride, limiting the detection wavelength range to near-infrared. Thus, extending a microfluidic waveguide sensing platform to mid- or even far-IR spectroscopy becomes highly desirable.

Chalcogenide (ChG) glasses are of great interest for microphotonics applications due to their structural flexibility, wide range of optical and electrical properties, large capacity for doping, high optical nonlinearity, and photosensitivity. Several microphotonics devices such as gratings [5], optical storage units [6], holographic recordings [7], optical amplifiers [8] and lasers [9], all of which utilize these unique properties of chalcogenides, have already been demonstrated. Chalcogenide glasses exhibit a wide transparency window stretching from the visible to the far-infrared, a property related to the large atomic mass of chalcogens and relatively weak bonding between the constituent atoms [10]. This special property makes chalcogenide glasses an ideal material candidate for sensing, as most chemicals and biological

#78720 - $15.00 USD Received 4 January 2007; revised 5 February 2007; accepted 19 February 2007

toxins which need to be detected have their spectral fingerprints in the mid and far-infrared range. Compared to their fiber-form counterparts [11, 12], planar ChG-based waveguides are more mechanically robust and amenable to large-scale integration with other on-chip photonic and electronic devices, enabling a full spectrum of optical signal read-out and processing functions. Chalcogenide waveguides have been fabricated in several glass compositions using techniques including direct laser writing[13], wet etching [14], plasma etching [15] and lift-off [16], and their applications in gas sensing have also been reported [17].

In this paper, we report, for the first time, the fabrication and characterization of a microfluidic sensor device integrated with planar chalcogenide waveguides. We also demonstrate the feasibility of using this sensor to detect N-methylaniline.

2. Device fabrication

2.1 Film deposition

Bulk $Ge_{23}Sb_7S_{70}$ glass was prepared from high purity elements using a traditional chalcogenide melt-quenching technique. Details of the bulk sample preparation process may be found elsewhere [15]. The high-quality glass bulk was then thermally deposited onto 6" Si wafers already coated with a 3 μm thermal oxide layer (Silicon Quest International Inc.) in a custom-designed thermal evaporator (112 Evaporator-Sputter Station from PVD Systems Inc.). The film was deposited at a base pressure of 2×10^{-7} Torr using a Tantalum baffled source, and the deposition rate was stabilized at 18 Å/s. The Si substrate was mounted on a thermostat stage and was thus maintained at room temperature throughout the deposition process.

2.2 Waveguide patterning and channel definition

Channel waveguides with a 6 μm width and a 400 nm height were defined using traditional lithography, and patterned subsequently via SF_6 plasma etching (Plasmatherm dual chamber etcher, gas flow 40 sccm, pressure 30 mTorr, incident power 350 W). Figure 1 schematically illustrates the fabrication process flow for our device. Excess photoresist was stripped off using oxygen plasma in the same plasma chamber. Details of the waveguide fabrication and characterization will be published shortly [16]. In a second photolithography step, microfluidic channels as well as fluid reservoirs were defined in a 25 μm-thick layer of SU8 (SU8 2025, Microchem Inc.) photocurable resin that was spun coated onto the wafer. The SU8 channels were then sealed using a PDMS (polydimethylsiloxane) cover. Before bonding, the wafer was cleaved into 12 mm × 8 mm dies. Due to differences in chemical composition, PDMS cannot be irreversibly bonded onto SU8 even after oxygen plasma surface treatment. To improve the adhesion between PDMS and SU8, a two-stage curing procedure was employed. PDMS monomer (Sylgard 184 Silicone Elastomer Kit, Dow Corning Inc.) was mixed with its curing agent at a 15:1 ratio. The mixture was degassed in a dessiccator and then partially cured at 65˚C for 1 h. Partially cured PDMS exhibits improved adhesion to SU8 due to uncross-linked dangling bonds on partially cured PDMS surface. Fluid inlet and outlet holes were punched into the PDMS cover using a syringe prior to its bonding to SU8 channels. Finally, the assembled device was heated at 65˚C for 3 h to fully cross-link the monomer to form the polymer. Plastic tubing systems were added to the liquid inlet and outlet to allow pressure injection of fluids. Figure 2 shows a photo of the assembled microfluidic chip with fluid inlet and outlet tubing.

#78720 - $15.00 USD Received 4 January 2007; revised 5 February 2007; accepted 19 February 2007

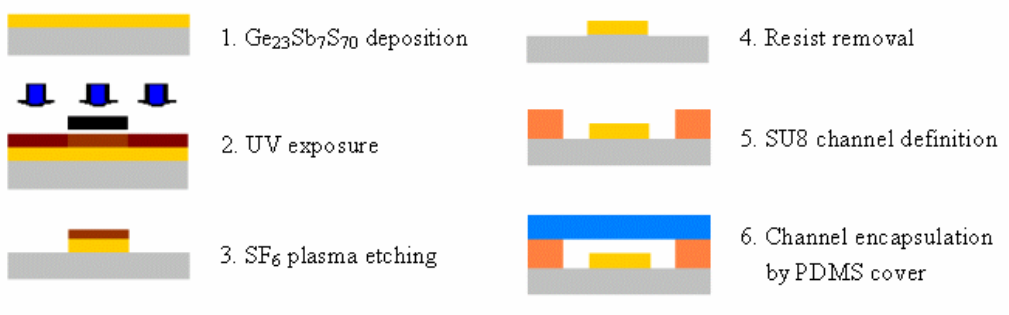

Fig. 1. Schematic processing flow of the microfluidic sensor chip integrated with $Ge_{23}Sb_7S_{70}$ waveguides.

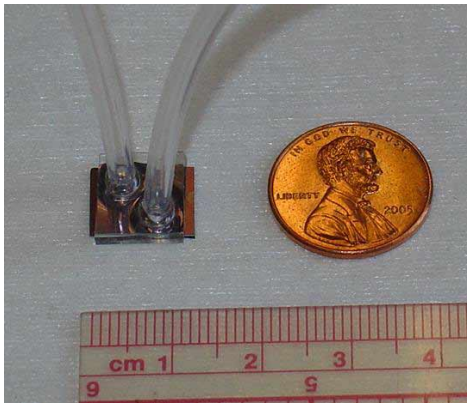

Fig. 2. Photo of the assembled microfluidic chip with fluid inlet and outlet tubing; the microfluidic channels and $Ge_{23}Sb_7S_{70}$ waveguides are too small to resolve in the image.

3. Experiment and results

3.1 $Ge_{23}Sb_7S_{70}$ film

A small film thickness is desirable, since a large fraction of the optical power then strays outside the glass core as an evanescent field. Since the waveguides have a small core height of 400 nm (compared to the 1550 nm wavelength), the interaction of the optical mode with the fluidic analyte surrounding the waveguide is enhanced, leading to improved sensitivity of the evanescent sensor.

For this reason, $Ge_{23}Sb_7S_{70}$ film has been deposited with a 400 nm ± 2.5% thickness across the entire 6" wafer. The thickness of the film was measured using a Tencor P10 surface profiler. Using a Metricon 2010 Prism Coupler, the refractive index of the as-evaporated film was determined to be (2.24 ± 0.02) at 1550 nm.

3.2 $Ge_{23}Sb_7S_{70}$ waveguide transmission loss

$Ge_{23}Sb_7S_{70}$ waveguide transmission loss was measured using paper-clip waveguide patterns defined on the same wafer as the sensor devices. $Ge_{23}Sb_7S_{70}$ waveguide transmission characterizations were performed on a Newport AutoAlign workstation. Lens-tip fibers were used to couple laser light into and out of the waveguides. Reproducible coupling between waveguides and fibers was achieved via an automatic alignment system. A schematic of the measurement setup is shown in Fig. 3(a). The loss measurement yielded a transmission loss of (2.3 ± 0.3) dB/cm at 1550 nm wavelength for as-fabricated channel waveguides, a relatively low loss compared to the previously reported 10-15 dB/cm loss at 1540 nm in As_2Se_3 channel waveguides [19].

#78720 - $15.00 USD Received 4 January 2007; revised 5 February 2007; accepted 19 February 2007

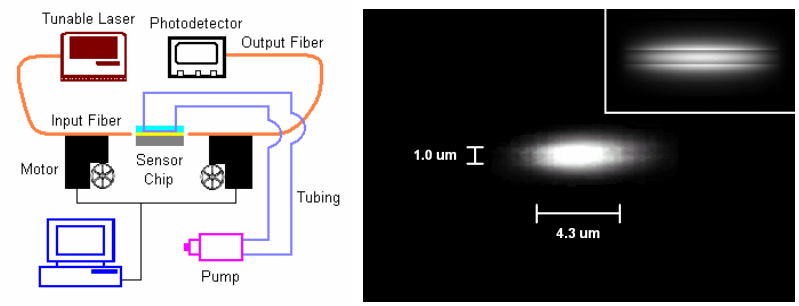

(a) (b)

Fig. 3. (a). Schematic of the measurement setup for transmission loss in waveguide and absorption in sensor; (b) Near field image of 1550nm optical output from a $Ge_{23}Sb_7S_{70}$ waveguide. The modal FWHM (Full Width at Half Maximum) is measured to be 4.3 μm by 1.0 μm. Inset: TM waveguide mode profile simulated using a finite domain technique[20].

3.3. Microfluidic channel and evanescent sensor

SEM cross-sectional images (taken on a JEOL 6320FV field-emission high-resolution SEM) of the waveguides in Fig. 4(a) exhibited a vertical sidewall profile and excellent feature size fidelity. In order to test the mechanical strength of the bonding between SU8 channels and the PDMS cover, FITC (fluorescein isothiocyanate, green fluorescence emission at 525 nm wavelength) solution was injected into the capped channels via pressure applied using a syringe. A fluorescence image in Fig. 4(b) (taken on an Olympus BX51 fluorescence microscope) indicates that the solution successfully filled the channels without leakage.

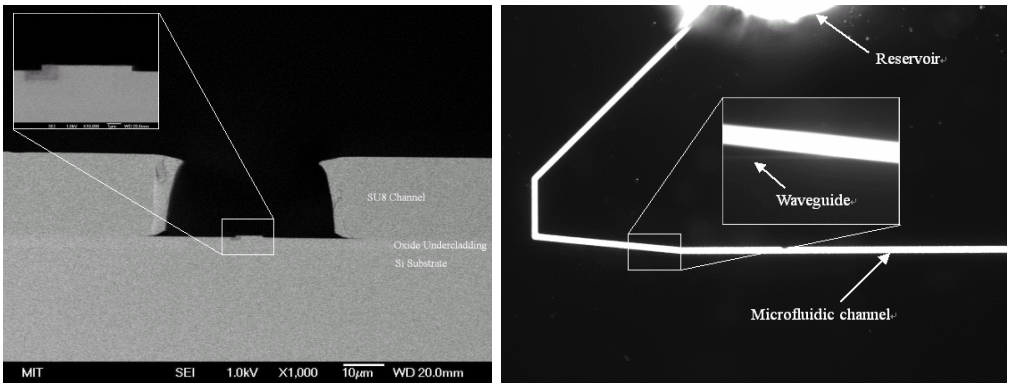

(a) (b)

Fig. 4. (a). SEM cross-section of a 50 μm wide SU8 microfluidic channel before being capped with a PDMS cover; Insets: the high magnification cross-sectional micrographs of the $Ge_{23}Sb_7S_{70}$ waveguides formed by SF_6 plasma etching sitting at the bottom of the channel, showing a vertical sidewall profile. The slightly darker area on the left side is an artifact due to electronic charge accumulation during SEM observation; (b) Fluorescent image of a microfluidic channel filled with FITC (fluorescein isothiocyanate) solution on a sensor chip, indicating successful fluid injection into the channel free of leakage.

Sensor performance was tested by monitoring the optical output while injecting a solution of N-methylaniline mixed with a solution of carbon tetrachloride into the microfluidic channel. The N-H bond in N-methylaniline is known to exhibit an absorption peak near 1500 nm [21], which was used as the characteristic fingerprint for chemical identification in our test. The absorption (in dB), αL, induced by N-methylaniline in our microfluidic channel was calculated by taking the ratio of light intensity transmitted through a microfluidic channel filled with pure carbon tetrachloride ($I_{solvent}$) and through a channel filled with N-methylaniline solution in carbon tetrachloride ($I_{analyte}$) (0.33, volumeric concentration), i.e.

#78720 - $15.00 USD Received 4 January 2007; revised 5 February 2007; accepted 19 February 2007

$$\alpha L = 10\log_{10}\frac{I_{solvent}}{I_{analyte}} \tag{1}$$

with L the length of the waveguide immersed in analyte solution (cm). The same waveguide was used throughout the experiment to eliminate any uniformity issue associated with waveguide intrinsic loss. The resultant absorption spectrum shown in Fig. 5(a) exhibits a well-defined absorption peak at 1496 nm, which is in excellent agreement with a traditional absorption measurement carried out on a Cary 5E UV-Vis-NIR dual-beam spectrophotometer as seen in Fig. 5(b). As seen in Fig. 5(b), since carbon tetrachloride has no absorption band and is transparent in the investigated range, this spectral peak is unambiguously assigned to N-H bond vibrational absorption.

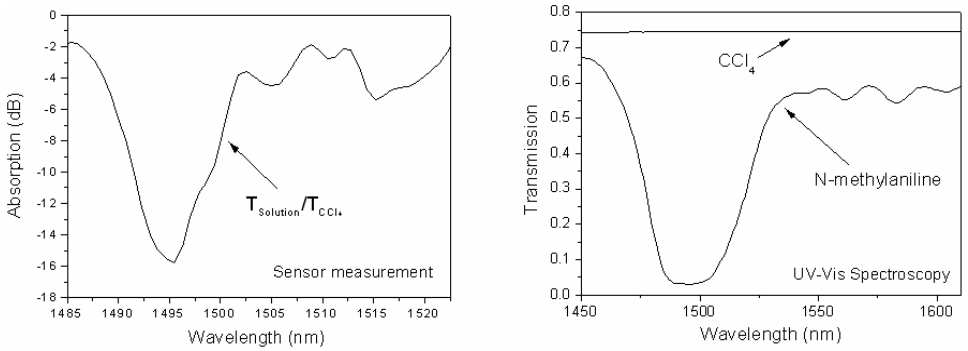

Fig. 5. (a). Absorption spectrum showing the N-H bond absorption at 1496 nm wavelength in N-methylaniline measured using our integrated evanescent sensor. The absorption is defined by taking the ratio of light transmission in the case of a microfluidic channel filled with pure carbon tetrachloride against the case when the channel is filled with N-methylaniline solution in carbon tetrachloride (0.33, volumetric concentration). (b) Transmission spectra of pure N-methylaniline and carbon tetrachloride (CCl_4) measured using traditional UV-Vis spectroscopy. The absorption spectrum of N-methylaniline shows the same N-H absorption peak near 1496 nm while carbon tetrachloride is transparent in the wavelength range of interest.

The peak absorption in dB at 1496 nm was measured for different concentrations of N-methylaniline solution in carbon tetrachloride and the result is shown in Fig. 6. The excellent linear fit suggests that the sensor exhibits linear response when varying analyte concentrations in the range investigated.

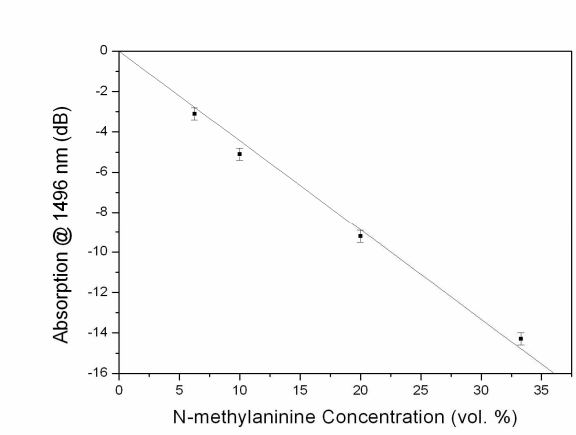

Fig. 6. Peak absorption of N-methylaniline solution in carbon tetrachloride measured using the waveguide evanescent sensor as a function of N-methylaniline volume concentration, indicating good linearity of the sensor response.

#78720 - $15.00 USD Received 4 January 2007; revised 5 February 2007; accepted 19 February 2007

Moreover, the absorbance at 1496 nm of a solution with a concentration of 0.33 volume % has been determined to be ~14.3 dB (signal) according to Fig. 5(a). As seen in Fig. 6, the sensor response is linear with concentration, and thus the absorption peak height scales with concentration. For this reason, at concentration x, the absorbance (dB) will be given by 14.3*(x/0.33). The noise induced by the power fluctuations has been estimated to be ~5% which corresponds to 0.21 dB. The minimum detectable concentration (denoted by x here) is reached when the signal is equal to the noise. For this reason, the sensor sensitivity to N-methylaniline in carbon tetrachloride is estimated to be 0.7% (given by 14.3*(x/0.33) = $\sqrt{2}$ *0.21) by comparing the absorption peak height (signal) with fiber output power. The lower limit actually measured in our experiment is 6.25% volumetric concentration.

5. Theory of the molecule detection mechanism for improvement of device performance

In the configuration we have adopted, the minimum detectable concentration of the analyte such as N-methylaniline (defined as the analyte concentration corresponding to a signal-to-noise ratio of unity) of waveguide evanescent sensors can be derived by comparing the sensor signal (output power decrease due to analyte absorption) to noise (signal output fluctuations) and thus is given as follows[22]:

$$c_{\min} = \frac{\sqrt{2}}{L\alpha\eta}\sqrt{(\frac{\Delta F_0}{F_0})^2 + (\frac{\sigma_j}{RF_0\exp(-AL)})^2} \qquad (2)$$

where R is the photodetector responsivity, F_0 is the input laser photon flux coupled into the waveguide, A stands for intrinsic waveguide loss not considering analyte absorption, L represents the length of the waveguide immersed in analyte solution, α is the absorption coefficient of pure analyte, η represents the waveguide power confinement factor in solution (i.e. fraction of optical power confined in analyte solution; note that it is different from the usual definition of confinement factor), and σ_j denotes dark current noise from the detector.

The terms in Formula (2) under the square root correspond to two major noise sources: input laser power fluctuation and photodetector noise at the output. The latter term is of significance only when the analyte solution has strong absorption or is highly concentrated, which limits the dynamic range of detection. The former term, i.e. fluctuation of input laser power, primarily stems from the spatial shift of input/output fibers in our case, which leads to approximately a 5% fluctuation of optical power effectively passing through the analyte solution.

As an example for the application of formula (2), if we utilize the strong absorption peak of water at 3 μm (α = 3333 cm^{-1} [23]) for detection of water in some non-absorbing solvent, the relevant minimum detectable concentration for our present sensor setup will be ~16 ppm for an interaction length of 1 cm, which improves further when the interaction length increases. The relatively low sensitivity (minimum detectable concentration ~0.7%) measured experimentally in the case of N-methylaniline is due to its low absorption coefficient at 1496 nm compared to that of water at 3 μm. Using mid-infrared probing wavelength, which is highly absorbed in the medium, could significantly enhance sensor performance. Formula (2) suggests that in order to further improve the output signal from the sensor, high input optical power F_0, small waveguide intrinsic loss A, and a large evanescent field η, are desirable. A moderately long waveguide immersed in solution will enhance sensitivity as well. However, the maximum waveguide length is limited by its intrinsic loss and photodetector noise.

For commercial chemical sensing applications, a more robust coupling scheme would be necessary to improve our current sensor configuration. One solution to eliminate coupling variations is to use one reference beam in a Y-splitter, which is not subjected to interactions with analyte solution, as a coupled power monitor. The concept is schematically demonstrated in Fig. 7. The input waveguide has to be single-mode so the ratio of power partition in the two beams is independent of coupling conditions. Following a derivation process similar to that used to obtain formula (2), absorption arising from analyte would thus be given as:

#78720 - $15.00 USD Received 4 January 2007; revised 5 February 2007; accepted 19 February 2007

$$\alpha L = 10\log_{10}\frac{(I_{sensor}/I_{ref})_{solvent}}{(I_{sensor}/I_{ref})_{analyte}} \text{ (in dB)} \quad (3)$$

where I_{sensor} and I_{ref} are output power from sensor beam and reference beam, respectively, and the subscripts "solvent" and "analyte" denote the cases when there is only pure non-absorbing solvent and when there is analyte solution present in the microfluidic channel, respectively. Significantly, equal power distribution in the two beams is not a necessary condition due to the fact that optical power only shows up in the expression in the form of ratios.

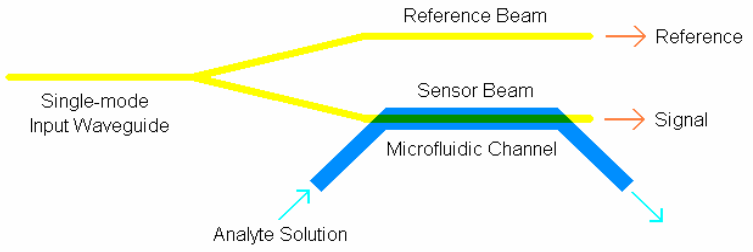

Fig. 7. Schematic illustration of a fabrication method to eliminate optical coupling related fluctuation within our microfluidic channels: Input laser beam goes through a single-mode waveguide and then a Y-splitter; output power from the reference beam is used as a monitor for coupling variations.

5. Conclusion

We have experimentally demonstrated the first chalcogenide waveguide evanescent sensor integrated with microfluidic channels for analyte transport. $Ge_{23}Sb_7S_{70}$ channel waveguides patterned by SF_6 plasma etching show a minimum loss of 2.3 dB/cm at 1550nm. The assembled device has been tested for N-methylaniline sensing, and the resultant transmission spectra exhibit a clear absorption band at 1496 nm, which, in agreement with traditional UV-Vis spectroscopy, corresponds to N-H bond absorption fingerprint. The sensor performance has been theoretically analyzed and a practical method for noise reduction has been proposed. Given the small size, high robustness, low-cost fabrication and good sensitivity, the sensor can find applications such as environmental monitoring and explosive detection.

Acknowledgment

This paper is based upon work supported by the Department Of Energy under Award Number DE-SC52-06NA27341. The authors would like to thank Pan Mao and Micro/Nanofluidic BioMEMS group at MIT for technical assistance and helpful discussions. The authors also acknowledge Microsystems Technology Laboratories at MIT and Center for Materials Science and Engineering at MIT for fabrication and characterization facilities.

Disclaimer

This paper was prepared as an account of work supported by an agency of the United States Government. Neither the United States Government nor any agency thereof, nor any of their employees, makes any warranty, express or implied, or assumes any legal liability or responsibility for the accuracy, completeness or usefulness of any information, apparatus, product or process disclosed, or represents that its use would not infringe privately owned rights. Reference herein to any specific commercial product, process, or service by trade name, trademark, manufacturer, or otherwise does not necessarily constitute or imply its endorsement, recommendation, or favoring by the United States Government or any agency thereof. The views and opinions of authors expressed herein do not necessarily state or reflect those of the United States Government or any agency thereof.

#78720 - $15.00 USD Received 4 January 2007; revised 5 February 2007; accepted 19 February 2007